Application of reactor dosimetry techniques for source term validation in F-18 production with a medical cyclotron

Joerg Konheiser[1,*] and *Stefan E.* Mueller[1]

[1]Helmholtz-Zentrum Dresden-Rossendorf, 01328 Dresden, Germany

Abstract. Imaging techniques such as positron emission tomography need radionuclides that can be produced with cyclotrons. The involved nuclear reactions mostly produce neutron and gamma radiation, which must be shielded. In order to be able to determine the required thickness of the shielding for a newly bought medical cyclotron, corresponding radiation protection calculations were carried out. The necessary neutron source term was supplied by the manufacturer. To verify this source term, additional source terms were calculated with the MCNP6 and the FLUKA code packages. The results with the source, on base of code internal nuclear models, produced comparable results, but the neutron yield with the source supplied by the manufacturer turned out to be lower by a factor of about 5. To validate the results, experiments were carried out on an already existing cyclotron. Neutron fluence was measured with standard monitors which are used in reactor dosimetry. The experiments were performed during regular ^{18}F production. Activities of the nuclides were measured by gamma spectroscopy and compared with the calculated activities.

1 Introduction

Imaging techniques are one of the mainstays of diagnostics in modern medicine and the positron emission tomography (PET) is nowadays established as a standard instrument. Cyclotrons are often used to produce the required radionuclides. In this technique, different nuclides are bombarded with protons or deuterons, which trigger nuclear reactions. Besides the desired nuclide, the initiated nuclear reactions also produce neutron and gamma radiation, which must be shielded. It can be assumed that this is the main source of radioactive dose rate when operating a cyclotron and therefore this radiation determines the thickness and design of the shielding. In addition, the neutron radiation leads to activation of the construction and building materials, which could be important for the decommissioning of the facilities. Therefore, the correct determination of the neutron and gamma source terms is a fundamental condition for a successful shielding calculation and thus for a sufficient protection of the staff during operation as well as during decommissioning.

* Corresponding author: j.konheiser@hzdr.de

There are different approaches to obtain the required source terms for the shielding calculations. In one approach, with which the source was probably also determined by the manufacturer, the energetic source spectrum is determined with the help of nuclear model programmes such as ALICE-91 [1]. The absolute number of neutrons emitted is determined based on tabulated yield rates assuming complete absorption of the beam. These are available in tabular form for many reactions for different proton energies and a standard current [2]. In this approach, however, it is assumed that the neutron source term originates exclusively from the desired reaction. The support documentation for an ACSI TR-FLEX cyclotron [3] refers to corresponding papers. Unfortunately, the primary reference is a private information [4].

Another approach is the direct calculation of the neutron and gamma source terms including all involved reaction channels within the radiation transport calculation itself. Today, modern radiation transport codes have the possibilities to simulate the transport and nuclear reactions of different particles within one calculation. In the programme MCNP6 [5], different nuclear models are integrated that can calculate the reaction channels of nuclear reactions and thus also the production of neutrons and gammas.

For the first shielding calculations for the new cyclotron [6], the neutron source term was specified externally, which was provided by the manufacturer and determined with the help of corresponding yield tables. In further calculations, the proton beam was then directly used as the source term in the calculations. This was required because no reliable source term data were available for the maximum proton beam energies of 28 MeV. The dose rate calculations showed big discrepancies in the results when using the proton-beam-based calculations with respect to calculations based on the manufacturer's source term.

The calculated source terms also show a large difference to the values determined with the approach based on tabulated activities. Therefore, the calculations were repeated with an independent programme. For these calculations, the code FLUKA [7, 8] was used, which uses different nuclear models for the calculation of the reactions respect to MCNP6. The calculation with this program gave similar results to MCNP6 and the results were published and discussed in [6]. To validate the results, experiments were subsequently carried out at the 18 MeV cyclotron of the HZDR, which was still in operation at the time. First results have already been published in [9]. In this paper, further experimental results of neutron fluence measurements with the help of activation monitors are presented. For these measurements, existing experience from the field of reactor dosimetry was applied.

2 The neutron source term

In addition to the validation calculations, a simplified model was developed to calculate the neutron source. This consists of a cylinder with a radius of 0.55 cm and a length of 4 cm, which is filled with 97% ^{18}O enriched water. This dimension corresponds to a typical irradiation volume as often used at the IBA cyclotron. The proton beam hits the front surfaces of the cylinder perpendicularly and will be absorbed along the axis of the cylinder. The emitted neutrons and their energy spectrum are determined on the surface of an empty sphere with a radius of 10 m. This allows geometric effects due to the target to be eliminated. This model was developed with both MCNP6 and FLUKA and corresponding calculations were carried out.

Since the exact shape of the proton beam is unknown, two approximations were calculated. In the first case, the proton beam was simulated as an infinitely small point beam; in the second case, a circular beam with a Gaussian distribution with a standard deviation of 0.125 cm was chosen. Since identical results were obtained for both approximations, a point proton beam was used for the comparative simulations.

As a standard, the generation of neutrons in the target was carried out using nuclear physics models. FLUKA uses a pre-equilibrium cascade model (PEANUT) [10] for the nuclear interactions and MCNP a cascade exciton model (CEM) [11].

In addition, MCNP6 calculations were carried out with nuclear data of the (p,n) reaction. The ^{18}O data are not included in the standard library of MCNP6. Therefore, these were generated based on the nuclear data library TENDL [12] with the programme NJOY [13]. TENDL is a nuclear data library that contains reaction cross sections calculated using the TALYS [14] nuclear model code system. Use of external cross sections is not possible in FLUKA.

Another difference in the consists in the cross-section data libraries used. In FLUKA the ENDF/B-VIIIR0 [15] library (except for lutetium, for which TENDL19 was used) was used and in MCNP6 the ENDF/BVII.1 library [16].

Fig. 1 shows both the proton and neutron fluences per primary proton. The plot is based on FLUKA simulation calculations. The protons only penetrate about 0.5 cm into the water target. Most of the protons are absorbed within the water target and only a small part is scattered back. Practically no protons are emitted over the other surfaces of the target. As expected, the neutrons are generated along the path of the proton beam in the water and leave the target approximately isotropically. For a proton current of 1µA, the integral over the energy spectrum gives a total neutron yield of 3.21×10^{10} n/s for the FLUKA calculation and 2.99×10^{10} n/s for MCNP6. The approximately 7% higher yield for the FLUKA calculations was already observed in [9] for protons at 24 and 28 MeV and is attributed to the differences in the basic nuclear physics models. In contrast, these calculated values are a factor of 3 higher than the value in [17], which is given as $1.115\text{x}10^{10}$ n/s for 1µA proton current. We suspect that the difference is due to additional neutron-generating reaction channels opening at 18 MeV proton energy. This was already suggested in [18].

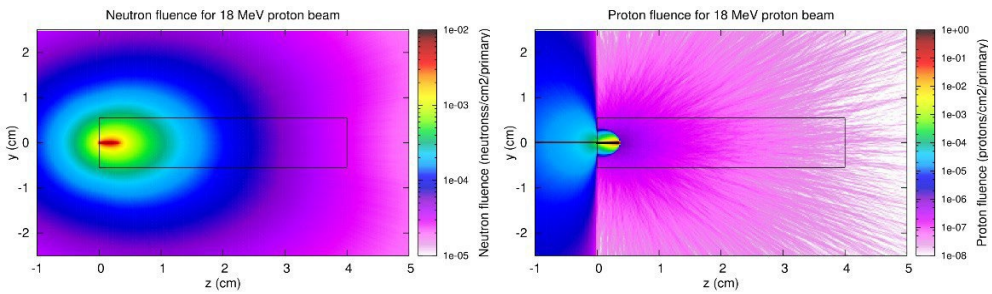

Fig. 1. Proton and neutron fluence distribution of an ^{18}O water target during irradiation with 18 MeV protons and with the simple model (taken from [9]).

3 Radiation field measurements with fluence monitors

For many years, an 18 MeV cyclotron has been operational at the HZDR, facilitating the production of various radionuclides. This could be used to validate the calculated source term. During a routine run to produce ^{18}F, activation foils were placed on the water target and the activities were measured after the end of the irradiation. The measured activities were subsequently compared with the calculated activities determined using the Monte Carlo transport codes MCNP6 and FLUKA. Unlike [9], we used the official FLUKA version 2021.2.9[19] for these studies, which contains updated information on branching ratios to metastable states using the JEFF-3.1A activation library [20] and has an improved treatment of low-energy neutrons by using pointwise cross sections.

3.1 Experimental setup

Fig. 2 shows the individual activation monitors that were irradiated together in one package and their position on the irradiation tank at the cyclotron. As can be seen, two stacks are irradiated at a time. This allowed two independent measurements for the sample

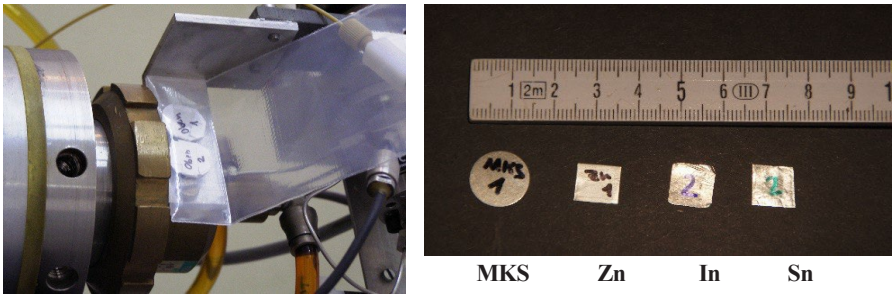

Fig. 2. The stacks of activation monitors placed on top of the irradiation header and examples for activation monitors (taken from [9]).

activation analysis. The monitor samples consist of four different metal foils, three pure metals and one alloy. In this paper, only the results of the alloy will be discussed. Table 1 shows the composition, the reactions with the nuclides produced, the energetic threshold of the reaction and the half-life of the MKS monitor alloy. This MKS monitor alloy was specially developed for experimental neutron flux analysis at fission reactors for power determination, as well as fluence measurements for validation of results in reactor dosimetry. The uncertainties in the composition are specified with 0.1%. This use of the MKS monitor makes sense because the energy spectrum of the neutrons is similar in quality to that on the outside of a reactor pressure vessel. The option of measuring the samples directly after irradiation made it possible to use additional nuclides than the usual ones for the comparison.

Table 1. Composition of the MKS monitor with the studied activation reactions, threshold energy of reaction and corresponding half-life.

Mass fraction	Reactions	Threshold	Half-life
81.63% Ni	^{58}Ni(n,np)^{57}Co	8 MeV	271.74d
	^{58}Ni(n,2n)^{57}Ni	12 MeV	1.48d
	^{58}Ni(n,p)^{58}Co	0.4 MeV	70.86d
	^{64}Ni(n,g)^{65}Ni	therm.	2.52h
15.16% Mo	^{98}Mo(n,g)^{99}Mo	therm.	2.75d
	^{100}Mo(n,2n)^{99}Mo	8 MeV	2.75d
	^{92}Mo(n,p)^{92m}Nb	2 MeV	10.15d
	^{100}Mo(n,g)^{101}Mo→^{101}Tc	therm.	14.2 min
2.62% W	^{186}W(n,g)^{187}W	therm.	23.72h
0.26% Mn	^{55}Mn(n,g)^{56}Mn	therm.	2.58h
0.31% Au	^{197}Au(n,g)^{198}Au	therm. (4eV)	2.69d
	^{197}Au(n,2n)^{196}Au	8 MeV	6.17d

Due to the different threshold energies of the reactions, it is possible to validate different regions in the spectrum. The location of the monitor packages, which was directly on top of the water tank, guaranteed a high neutron flux and thus a high reaction rate. On the other hand, this meant that the water tank had to be modelled very precisely in the calculations in order to cover the geometric influences. The irradiation took place during a regular ^{18}F production. The energy of the protons was 18 MeV at an average beam current of 25 µA and the irradiation lasted 50 minutes.

The activation measurements presented here were carried out in the "Environmental Monitoring Department" of the "VKTA - Strahlenschutz, Analytik & Entsorgung Rossendorf e. V. The activity determination was performed by gamma spectrometry using high purity germanium detectors. The detectors used typically have an efficiency of about 44% relative to a 3" x 3" NaI(Tl) detector and with a resolution of 1.78 keV at 1332 keV. The detectors are calibrated weekly against a certified standard. In order to detect nuclides with relatively short half-lives, some of the activation monitors were examined as early as about one hour after the end of irradiation (EOI). For nuclides with longer half-lives, repeated measurements were possible. The activity values were provided both for the time of measurement and for the EOI (the values were extrapolated accordingly using the half-life values). However, previous studies have found that these extrapolations were not always reliable, especially when a nuclide is produced with delay from an excited state. The uncertainties reported by laboratory were between 5% and 25%, depending on the reaction channel.

3.2 Calculation of the activation of the fluence monitors

Fig. 3 shows the geometry models of MCNP6 and FLUKA. A strong effort was made to ensure that the structure of the water tank and the surrounding cooling body corresponded to reality in detail. One problem was that the exact compositions and densities of the materials were not known and therefore standard data was used. In the models, the flange of the beam tube adapter and the surrounding walls were not considered, since it is assumed that the influence of backscattered neutrons on the activation of the monitors is negligible.

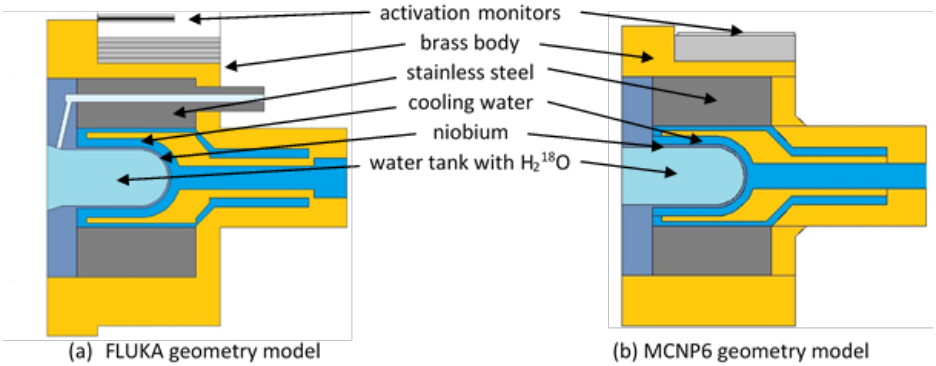

Fig. 3. Geometry models of MCNP6 and MLUKA (taken from [9]).

Despite a small number of differences, it has been assumed that the geometry models in the FLUKA and MCNP6 calculations are consistent. As a result, any differences in the calculated results are attributable to the radiation transport models and / or nuclear data. An example of one of the geometrical differences is the fine injection pipe that was modelled explicitly in the FLUKA model but smeared in the MCNP6 model. The difference is expected to have only a marginal influence on the calculated results of the monitors.

The stacks of monitors were also modelled according to the respective position. The weight of the individual monitors was measured and by using the known geometry an average density of the used monitor materials was determined. These average densities were then used for the simulation. The source term in the simulations, as already written above, consisted of a point proton beam with a kinetic energy of 18 MeV. Fig. 4 shows the neutron fluence on the axial section plane of a FLUKA simulation. The proton stopping peak directly after the penetration of the protons into the water and the practically isotropic emission of the neutrons can be clearly seen.

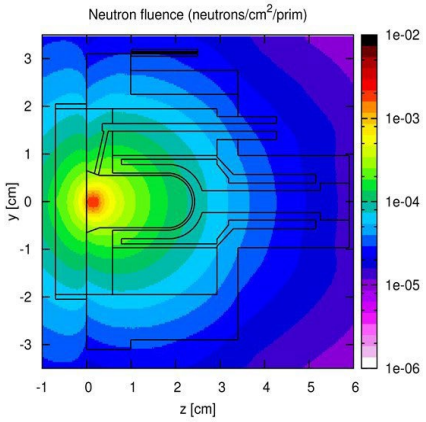

Fig. 4. Neutron fluence in neutrons/cm^2/ primary proton in the irradiation header (calculated with the FLUKA) (taken from [9]).

The activities $A_m(t_{meas})$ at a time t and for a produced nuclide can be determined with a known neutron flux rate and irradiation time with the following equation:

$$A_m(t)=\Sigma_i [\rho_n * V * \lambda_m * \delta_{ni} * \Phi_i * t_{irr} * (1 - e^{-\lambda_m * t_{irr}}) * e^{-\lambda_m * t_d}] \quad (1)$$

Here ρ_n is the nuclear density of the monitor (nuclei/barn cm), V is the sample volume (cm^3), δ_{ni} is the group cross-section of the (n,x) reaction (barn) from monitor, Φ_i is the group flux (neutrons/s/cm^2), t_{irr} is the irradiation time (s), t_d is the time between EOI and measurement time (s) and λ_m is the decay constant of the active nuclide (1/s).

For MCNP6, equation 1 was used to determine the activities. The necessary cross-section data were generated with the program NJOY. This made it possible to fit the calculated neutron flux over cross- sections from different nuclear data libraries and to estimate systematic uncertainties resulting from the available cross-section data sets. For some nuclides, cross-sections were only present in one library. The transportation calculation of MCNP was only carried out with ENDF/BVII.1 data.

In contrast, the activities in the FLUKA calculations were determined directly, so that the same data (ENDF/B8.0) was used for both transportation and activity determinations. Using the irradiation time profile, FLUKA can calculate the resulting nuclide activities in Bq/cm^3. For selected geometry regions, the current activities can be output in a table for any point in time. The disadvantage is that the cross-section data are fixed in the FLUKA program and cannot be changed by the user.

3.3 Results and Discussion

Table 2 shows the results for the measured and simulated activities for the MKS monitor at the corresponding measurement time. The experiment was carried out three times. Samples were irradiated on 11 August 2016 (A), 29 September 2016 (B) and 13 February 2017 (C). The results are listed in the table with the corresponding labels A, B and C. The materials for the monitors were used from the same batches and therefore are identical in the composition for the different irradiation times. Measurement uncertainties of 6% up to 22% were given by the "Department of Environmental Monitoring". The statistical uncertainty of the simulations was less than 15%. The errors of the MCNP values are based on the statistical errors of the neutron spectra. Except for energy cutting, no other techniques to reduce the variance of MCNP and FLUKA codes were used in this work. For the threshold monitors, special calculations were carried out in the high-energy groups, which can be clearly seen in the errors. FLUKA directly determines the error of the activities. The table shows the MCNP6 results of multicomponent monitor using the component monitor using the ENDF/BVII.1 nuclear data library [16] and, where no data were available, those using the JEFF3.1 or JEFF3.1A nuclear data library [20]. Of course, the experimental results were also compared with results obtained with other libraries. In most cases, however, these did not differ from those with ENDF/BVII.1. The IRDF (International Reactor Dosimetry File) data were not used in this work.

Table 2 presents the results for the multicomponent monitor. With the exception of the nuclide activities of the reactions from ^{58}Ni(n,np)^{57}Co, ^{58}Ni(n,2n)^{57}Ni and ^{197}Au(n,2n)^{196}Au, the FLUKA and MCNP6 calculations reproduces the experimental results relatively well. The C/E ratios (calculation/experiment) range from 0.56 to 2.36, i.e., a difference of around 100% both downwards and upwards was calculated. Two thirds of these C/E ratios have deviations smaller than 30%. MCNP6 gives results that are about 20% lower than the FLUKA results, except for ^{58}Co and ^{92m}Nb production. It should be noted that for both reactions JEFF3.1a data was used to calculate the activities. The lower values obtained with the MCNP6 code compared to the FLUKA results correlate with the results on the source term in section 2 and thus are mostly explainable by this. On average, the C/E ratios from MCNP6 are slightly less than one and those with FLUKA are slightly bigger than one, so when averaged over all C/E ratios, a value is calculated close to one.

Table 2. Measured and calculated activities of the MKS monitor and the C/E ratios (the thermal reactions are greyed on the background).

		Activities in Bq				**C/E**		
reaction		**Meas.**	**MCNP6**		**FLUKA**	**MCNP**	**FLUKA**	**C_M/C_F**
^{55}Mn(n,g)^{56}Mn	B	**190 (8%)**	**167 (1%)**	B7	**239 (15%)**	**0.88**	**1.26**	**0.70**
	C	**140 (8%)**	**131 (1%)**	B7		**0.94**		
^{58}Ni(n,np)^{57}Co	A	**4.2 (11%)**	**0.7 (<1%)**	B7	**1.03 (7%)**	**0.17**	**0.24**	**0.68**
	B	**7.7 (11%)**	**0.91 (<1%)**	B7	**1.57 (7%)**	**0.12**	**0.20**	**0.58**
	C	**4.2 (11%)**	**0.69 (<1%)**	B7	**0.74 (7%)**	**0.16**	**0.18**	**0.93**
^{58}Ni(n,2n)^{57}Ni	A	**3.5 (14%)**	**2.37 (<1%)**	B7		**0.68**		
	B	**15 (14%)**	**3.1 (<1%)**	B7	**1.43 (15%)**	**0.21**	**0.10**	**2.17**
	C	**6.8 (14%)**	**2.34 (<1%)**	B7	**2.28 (15%)**	**0.34**	**0.34**	**1.03**
^{58}Ni(n,p)^{58}Co	A	**280 (6%)**	**370 (<1%)**	Jeff3.1a	**320 (<1%)**	**1.32**	**1.14**	**1.16**
	B	**450 (6%)**	**346 (<1%)**	Jeff3.1a	**314 (<1%)**	**0.77**	**0.70**	**1.10**
	C	**330 (6%)**	**327 (<1%)**	Jeff3.1a	**255 (<1%)**	**0.99**	**0.77**	**1.28**
^{64}Ni(n,g)^{65}Ni	B	**80 (22%)**	**132 (<1%)**	B7	**138 (15%)**	**1.65**	**1.73**	**0.96**
	C	**8.4 (22%)**	**18.4 (<1%)**	B7	**19.8 (15%)**	**2.19**	**2.36**	**0.93**
^{92}Mo(n,p)^{92m}Nb	C	**7.5 (11%)**	**8.14 (<1%)**	jeff3.1a	**6.65 (15%)**	**1.09**	**0.89**	**1.22**
^{99}Mo production	A	**86 (7%)**	**103 (<1%)**	B7	**197 (6%)**	**1.20**	**2.29**	**0.52**
	B	**240 (7%)**	**134 (<1%)**	B7	**206 (6%)**	**0.56**	**0.86**	**0.65**
	C	**120 (7%)**	**95.4 (<1%)**	B7	**118 (6%)**	**0.80**	**0.98**	**0.81**
^{101}Tc production	B	**230 (6%)**	**172 (<1%)**	B7	**296 (13%)**	**0.75**	**1.29**	**0.58**
^{186}W(n,g)^{187}W	A	**180 (6%)**	**204 (3%)**	jeff3.1	**288 (6%)**	**1.13**	**1.60**	**0.71**
	B	**340 (6%)**	**264 (3%)**	jeff3.1	**499 (6%)**	**0.78**	**1.47**	**0.53**
	C	**200 (6%)**	**168 (3%)**	jeff3.1	**239 (6%)**	**0.84**	**1.20**	**0.70**
^{197}Au(n,2n)^{196}Au	A	**3.3 (22%)**	**0.65 (<1%)**	jeff31a		**0.20**		
	C	**2.4 (22%)**	**0.65 (<1%)**	jeff31a	**1 (15%)**	**0.27**	**0.42**	**0.65**
^{197}Au(n,g)^{198}Au	A	**55 (6%)**	**53(7%)**	B7	**156 (7%)**	**0.96**	**2.84**	**0.34**
	B	**110 (6%)**	**68.5(7%)**	B7	**119 (7%)**	**0.62**	**1.08**	**0.58**
	C	**68 (6%)**	**49(7%)**	B7	**69 (7%)**	**0.72**	**1.01**	**0.71**

For the reactions ^{58}Ni(n,np)^{57}Co, ^{58}Ni(n,2n)^{57}Ni and ^{197}Au(n,2n)^{196}Au, both simulation codes consistently calculate activities that are too low by a factor of 4 to 8 (with one exception : ^{58}Ni(n,2n)^{57}Ni, Meas. A). All three reactions have a very high threshold (from 8 or 12 MeV) and low cross sections. Since the big discrepancy occurs in all three high-threshold reactions, it is assumed that the cause is a too small neutron source in this energy range. Independently of this, the results show a big statistical error. This can be seen in the large scatter when comparing the C/E ratios.

An interesting fact is that the activity was greater in a second measurement of ^{58}Co. The reason for this is that is a delayed production of ^{58}Co due to the presence of the meta-stable state ^{58m}Co. The half-life from ^{58m}Co is 9 hours.

3.4 Uncertainties in the calculations

The main uncertainty is the neutron source in the simulations and the resulting neutron flux rate at the sample positions and a second part the reaction cross sections. Spectrum studies show in [9] that uncertainties of the source term can be up to 50 % below energies of 1 MeV, depending on the nuclear model used. In contrast, the beam parameters can be determined very well, and their uncertainties are very small.

Also, the geometry models should not play a significant part. As mentioned in section 3.2, the two geometry models were implemented with great care, so that when comparing the simulation results with the measurements, these have only minimal effects and are limited to the influence of possible backscattering of neutrons from the surrounding walls. Uncertainties from the irradiation time regime and measurement time uncertainties can also be considered very minor and become negligible in the present study.

One basic ingredient for the determination of the reaction rates and thus the activities are the used data libraries for the reaction cross sections. By the fact that the activities of the MCNP6 calculations were determined separately the neutron flux calculations, different cross-section data libraries could be studied. The cross-section data were generated using the NJOY program. Cross section from ENDF/B-VII, JEFF3.1A, JENDL33, EAF2010, and ROSFOND2010 libraries were generated. Specified branching paths for isomeric states were also considered. In general, the cross sections agreed well at thermal energies, whereas bigger differences appeared at high energies and at resonances. For example, for some reactions, the ENDF/B-VII data delivered activation results about 30% higher than those calculated with the JEFF3.1A data. For majority of the reactions, the differences in activation results are on the order of 10%.

4 Conclusion and Outlook

Inspired by the calculations of a shielding design for a new cyclotron bunker at HZDR, investigations on the neutron source term for ^{18}F production were performed at an IBA cyclone 18/9 cyclotron using the Monte Carlo transport and reaction codes MCNP6 and FLUKA. The work here complements and extends the results already presented in [6]. In contrast to the first release, the official FLUKA version was used here. It was found that below 1 MeV, the nuclear models implemented in the MCNP6 code yielded a neutron production rate up to 50% smaller than that of FLUKA. The total neutron production for both codes was about three times higher than the value determined in [17] for ^{18}F production, which is broadly used for such shielding calculations.

To validate the results of the Monte Carlo codes, an accurate model of the water tank from Cyclone 18/9 for the two codes was developed and realized irradiation experiments were recalculated. These were performed during typical ^{18}F production runs. Small monitor sample foils of various metals and alloys were irradiated, and the resulting activities were measured. The activities were determined using gamma spectroscopy with HPGe detectors. The monitors were irradiated on three different irradiation days. In this paper, the results from the MKS monitors were presented, where the nuclides from 11 reactions were studied. A total of 26 comparisons were presented. The C/E ratios were in most cases between 0.7 and 1.3. In general, results calculated with the MCNP6 codes were up to 40% lower than those of the FLUKA calculation. The main cause for this effect is the source term. For three reactions, the Monte Carlo simulations consistently gave much lower results than the measured data (C/E ratio as low as 0.12 were observed). For these reactions, the uncertainties discussed cannot explain the discrepancies, so it is likely that the reaction cross sections are responsible for the results. Nevertheless, despite the sometimes-significant variations between experiment and calculation, the results show that the calculated neutron source terms using the nuclear models implemented in MCNP6 and FLUKA are better than those based solely on the ^{18}F yield [17], in any case for a proton beam of 18 MeV.

To consolidate our results, further experiments are planned at the new cyclotron of HZDR. In these experiments, both the target material and the proton energy will be varied. The goal is to provide validated absolute neutron fluence spectra for shielding calculations at medical cyclotrons.

The authors would like to thank S. Bartel of VKTA for providing the analysis of the sample monitors. We also like to thank S. Preusche and F. Hobitz of HZDR for assistance and support with the monitor irradiation at the cyclotron.

References

1. Blann, M., ALICE-91, Statistical Model Code System with Fission Competition. RSIC Code, PACKAGE PSR -146 (1991)
2. International Atomic Energy Agency (IAEA), Positron emitters for medical applications (2019), https://www-nds.iaea.org/medical/positron_emitters.html
3. Final Report Monte Carlo Simulation of TR 24 Shielding (Sherbrooke Project) documentation supplied with TR-FLEX cyclotron, Advanced Cyclotron Systems, Inc., Richmond, Canada (2011)
4. Bosko, A., General Electric Pettrace Cyclotron as a Neutron Source for Boron Neutron Capture Therapy, Dissertation, Texas A&M University 2005-11-01 (2005)
5. Goorley, T., et al., Initial MCNP6 Release Overview, Nuclear Technology 180, pp 298-315 (2012)
6. Konheiser, J., Naumann, B.; Ferrari, A.; Brachem, C.; Müller, S., Source Terms, Shielding Calculations and Soil Activation for a Medical Cyclotron, J. Radiol. Prot. **36** 819-831 (2016)
7. Ferrari, A., Sala, P.R., Fasso, A., Ranft, J., FLUKA, CERN-2005-10, INFN/TC 05/11, SLAC-R-773 (2005)
8. Böhlen, T.T., Cerutti, F., Chin, M.P.W., Fasso, A., Ferrari, A., Ortega, P.G., Mairani, A., Sala, P.G., Smirnov, G., Vlachoudis, V., Nuclear Data Sheets 120, 211-214 (2014)
9. Konheiser, J.; Müller, S. E.; Magin, A.; Naumann, B.; Ferrari, A., Source term calculation and validation for F-18 production with a cyclotron for medical applications at HZDR, J. Radiol. Prot. **39** 906-919 (2019)
10. Ferrari A., Sala, P.R., Proc. MC93 Int. Conf. on Monte Carlo Simulation in High Energy and Nuclear Physics, p.277-288, (1994)
11. Mashnik, S., Sierk, A., CEM03.03 User Manual, Los Alamos National Laboratory, Report LA-UR-12-01364 (2012)
12. Koning, A.J., Rochman, D., Sublet, J., Dzysiuk, N., Fleming, M., van der Mark, S., Nuclear Data Sheets 155 (2019)
13. MacFarlane, R., Kahler, A., 2010, Nuclear Data Sheets 111, pp. 2739-2890 (2010)
14. Koning, A.J., Rochman, D., Nuclear Data Sheets 113, 2841(2012)
15. Evaluated Nuclear Data File ENDF/B-VI.8, released in October 2001, (2001)
16. M.B. Chadwick et al., ENDF/B-VII.1, Nuclear Data Sheets Volume 112 Issue 12, p. 2887-3152 (2011)
17. International Atomic Energy Agency 2001, Report IAEATECDOC-1211 (2001)
18. L.R. Carrol, Presentation at the 9th Int. Workshop on Targetry and Target Chemistry, Turku, Finland, (23-25 May 2002)
19. F. Ballarini, at al., FLUKA: Status and Perspectives, Proceedings of the "15th Workshop on Shielding Aspects of Accelerators, Targets, and Irradiation Facilities" (SATIF-15), East Lansing, Michigan, USA, September 20-23, 2022
20. A. Koning, at al.,The JEFF-3.1 Nuclear Data Library - JEFF Report 21. NEA. (2014)